Interchain Expanded Extra-Large Pore Zeolites

Authors Zihao Rei Gao,[1,†,ł] Huajian Yu,[1,ł] Fei-Jian Chen,[2,ł] Alvaro Mayoral,[3,4] Zijian Niu,[2] Ziwen Niu,[5] Xintong Li,[5] Hua Deng,[6] Carlos Márquez-Álvarez,[7] Hong He,[6,8] Hao Xu,[5] Wei Fan,[9] Salvador R. G. Balestra,[1,‡] Jian Li,[10,*] Peng Wu,[5,*] Jihong Yu,[2,*] and Miguel A. Camblor[1,*]

Affiliations

[1]Instituto de Ciencia de Materiales de Madrid, Consejo Superior de Investigaciones Científicas (ICMM-CSIC), 28049 Madrid, Spain.

[2]State Key Laboratory of Inorganic Synthesis and Preparative Chemistry, College of Chemistry, International Center of Future Science, Jilin University, Changchun 130012, China.

[3]Instituto de Nanociencia y Materiales de Aragón (INMA), CSIC-Universidad de Zaragoza, 50009 Zaragoza, Spain.

[4]Laboratorio de Microscopias Avanzadas (LMA-Universidad de Zaragoza), 50018 Zaragoza, Spain.

[5]Shanghai Key Laboratory of Green Chemistry and Chemical Processes, School of Chemistry and Molecular Engineering, East China Normal University, Shanghai, 200062, China.

[6] Center for Excellence in Regional Atmospheric Environment, Key Laboratory of Urban Pollutant Conversion, Institute of Urban Environment, Chinese Academy of Sciences, Xiamen 361021, China.

[7]Instituto de Catálisis y Petroleoquímica, Consejo Superior de Investigaciones Científicas (ICP-CSIC), 28049 Madrid, Spain.

[8]State Key Joint Laboratory of Environment Simulation and Pollution Control, Research Center for Eco-Environmental Sciences, Chinese Academy of Sciences, Beijing 100085, China.

[9]Department of Chemical Engineering, University of Massachusetts, Amherst, MA 01003, USA.

[10]State Key Laboratory of Coordination Chemistry, School of Chemistry and Chemical Engineering, Nanjing University, Nanjing, Jiangsu 210023, China.

[†]Current address: Department of Chemical and Biomolecular Engineering and Institute for NanoBioTechnology, Johns Hopkins University, Baltimore, MD 21218, USA.

[‡]Current address: Departamento de Sistemas Físicos, Químicos y Naturales, Universidad Pablo de Olavide, Ctra. Utrera km 1, Seville 41013, Spain.

[ł] These authors contributed equally to this work.

Abstract

Stable aluminosilicate zeolites with extra-large pores open through rings of more than 12 tetrahedra are in demand to process molecules larger than those currently manageable. However, until very recently, [1,2,3] they proved elusive. Here we report a new strategy based on an interchain expansion design concept that yields thermally and hydrothermally stable silicates by expansion of a one dimensional (1D) silicate chain with an intercalated silylating agent that separates and connects the chains. As a result, new types of zeolites zeolites with extra-large pores delimited by 20, 16, and 16 Si tetrahedra along the three crystallographic directions, respectively, are obtained. The as-made inter-chain expanded zeolite contains dangling Si-CH_3 groups that by calcination connect to each other resulting in a true, fully connected 3D zeolite framework with a very low density, just slightly above that of water. Additionally, it features triple four ring units never seen before in any type of zeolite. Ti can be introduced in this zeolite to obtain a catalyst active in the liquid-phase oxidation of bulky alkenes that shows promise in the industrially relevant clean production of propylene oxide using cumene hydroperoxide as an oxidant.

Introduction

While zeolites typically crystallize as three-dimensional (3D) fully connected framework materials,[4] called tectosilicates when silica based,[5] there exist examples of layered zeolite precursors that only form the final zeolite by a postsynthetic 2D-3D topotactic condensation.[6,7] The 2D layered precursors have been shown to also offer the opportunity to produce expanded versions of the corresponding zeolite by an intralayer expansion reaction of the layered precursor with a silylating agent.[8,9,10] This reaction introduces Si atoms between the layers, thus increasing the number of Si members in the ring limiting the pores.[11] The obtained materials are called Interlayered Expanded Zeolites (IEZ), although we propose to use a different acronym, ILEZ, for reasons that will be obvious below. ILEZ materials are interrupted frameworks rather than true zeolites because dangling Si-R or Si-OH groups remain in the final as-made and calcined materials, respectively.[12,13] Very recently, we have reported the first case of a 1D-to-3D topotactic condensation of a complex chain silicate zeolite precursor (ZEO-2) into the extra-large pore ZEO-3 zeolite, which was at that time the silica polymorph of lowest density ever reported.[2] ZEO-3 has a 3D system of pores open through rings containing 16, 14, and 14 tetrahedra (16×14×14 membered ring, MR). Here we report that it is possible to introduce silicon between the chains of ZEO-2, resulting in what we call Interchain Expanded Zeolites (IChEZ). The resulting zeolites have a 3D system of extra-large 20, 16, and 16 MR and after calcination contains no dangling bonds, so it is a true fully connected tectosilicate zeolite that, additionally, contains triple 4-ring (T4R)

units never observed before. Introduction of Ti in ZEO-5 results in an extra-large pore catalyst for the selective oxidation of alkenes.

Synthesis and structure of the Interchain Expanded Interrupted Zeolites ZEO-4A and ZEO-4B

Fig. 1 illustrates the interchain expanded reaction process and the structure of the obtained zeolites, which were solved and refined by combining state-of-the-art 3D electron diffraction (3D ED) and synchrotron powder X-ray diffraction data (SPXRD). The reactions that introduce silicon between the chains of ZEO-2 (Fig. 1A) are carried out in acidic ethanolic solution using either dimethyldichlorosilane (DCDMS, containing a single Si per molecule) or 2,4,6,8-tetramethylcyclotetrasiloxane (TMCTS, a single 4-ring, S4R, containing four Si per molecule with methyl and H substituents at each Si corner). The reaction results in the intercalation of new silicon atoms in between adjacent chains connecting them together in a new stable crystalline zeolite (PXRD shown in Fig. 2C). The resulting materials, which we call ZEO-4A (Fig. 1B) and ZEO-4B (Fig. 1C), respectively, depending on the silylating agent used, DCDMS or TMCTS respectively, maintain the needle like morphology of ZEO-2 (Fig. S2). While our previous ZEO-1 to ZEO-3 materials were all developed and patented by the Anhui ZEO New Material Technology Co., China, the materials reported in this work have been developed in the ICMM-CSIC, Spain, but the same ZEO nomenclature has been used for convenience.

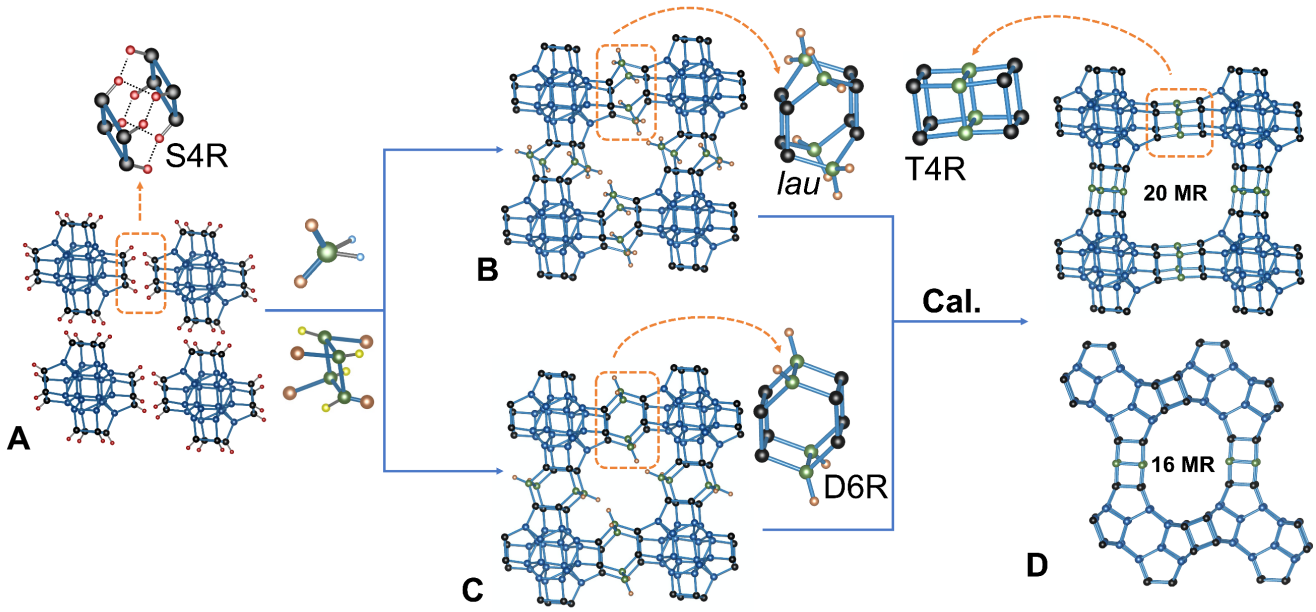

Fig. 1. Preparation and structure of ZEO-4A, ZEO-4B and ZEO-5. (**A**) starting from ZEO-2, a chain silicate with abundant hydrogen bonding between S4R, silylation with DCDMS or TMCTS produces the interchain expanded zeolites ZEO-4A and ZEO-4B (**B** and **C**, respectively), two interrupted zeolites that upon calcination yield the same true (*i.e.*, non-interrupted) zeolite, ZEO-5, containing a 3D system of extra-large 20×16×16 MR pores (**D**). In each structure, the relevant structural units are highlighted in an orange dash rectangle: the starting H-bonded S4R (**A**), are connected by D^2 (forming *lau* units **B**) or T^3 (forming double 6-ring units, D6R, **C**) Si atoms, which are fully connected by calcination into a new T4R (**D**). All the materials are shown approximately along the [001] direction. Bridging O atoms are omitted for clarity. Methyl groups are brown, chloride is light blue, hydrogen directly bonded to Si is yellow. In TMCTS, the conformation of methyl and H at each side of the ring is disordered. Si atoms are distinguished by color as Si that are always Q^4 (blue), Si that are Q^3 before the interchain expansion (black) and Si introduced during the interchain expansion reaction (green). All the Si atoms in (**D)** are Q^4.

The interchain expansion concept by insertion of DCDMS or TMCTS and the knowledge of the ^{29}Si magic angle spinning (MAS) nuclear magnetic resonance (NMR) in Fig. 2A of ZEO-4A (D^2 + Q^4) and ZEO-4B (T^3 + Q^4), respectively, see below, allowed us to model build the corresponding structures of both zeolites followed by optimization by density functional Tight Binding (TB) methods (see details in the supplementary information). Nonetheless, the single-crystal structure of both ZEO-4A and ZEO-4B was successfully solved *ab initio* by using continuous rotation electron diffraction (cRED). Thanks to the high-quality cRED data (Fig. S3-S4, Tables S1-S2, and S5), the positions of silicon and oxygen atoms on the framework structure of ZEO-4A and ZEO-4B were located directly from the observed electron density maps (Fig. S5), while some dangling Si-CH_3 groups were observed from the difference electron density map during the refinement against cRED data (Fig. S6). The resulting ZEO-4 materials contain nominally extra-large 20×16×16 MR pores and present two structurally different variants of the interchain expanded interrupted zeolite because of the different silylating reagents used. With DCDMS the silylating agent contains two methyl groups per Si and can connect only to the silica chains and not among them in ZEO-4A (Fig. 1B). However, TMCTS contains only a single methyl group per Si so the newly introduced Si atoms connect not only to the chains but are also interconnected in pairs through oxygen bridges in ZEO-4B (Fig. 1C). The final configuration of the newly introduced Si in ZEO-4B implies the breaking of the TMCTS ring in the acid alcohol solution. In both ZEO-4 materials, the dangling Si-CH_3 groups should effectively reduce the pore apertures and provide a four-lobed shape of the windows along [001] further reducing the effective entrance (Fig. S17). To obtain more accurate

atomic positions, the structures of ZEO-4A and ZEO-4B, including the position of the dangling Si-CH_3 groups, were subsequently Rietveld refined against SPXRD (Fig. S10, Table S7-S11).

MAS NMR

The ^{29}Si MAS NMR spectra of ZEO-4A and ZEO-4B demonstrate the insertion of the silylating agents in both materials, as they show either D^2 [*i.e.* Si(OSi)$_2$(CH$_3$)$_2$ at -16 and -13 ppm] or T^3 [*i.e.* Si(OSi)$_3$(CH$_3$) at -65 and -63 ppm] resonances, respectively (Fig. 2A). The reason for the double resonances is that the silanes exist in two different crystallographic sites in both materials. All remaining resonances are assigned to Q^4 species [*i.e.* Si(OSi)$_4$ in the range of -108 to -114 ppm] indicating that the originally abundant Q^3 [*i.e.* Si(OSi)$_3$OH or Si(OSi)$_3$O$^-$] species in ZEO-2 have essentially all been connected to the newly inserted Si.[2] Additionally, ^{13}C MAS NMR shows mainly resonances assigned to the methyl groups at -3 and -8 ppm for ZEO-4A and ZEO-4B (Fig. S14a), respectively, and only in ZEO-4B trace amounts of ethanol can be deduced by the presence of very small resonances at 16 (-CH$_3$) and 58 (-CH$_2$OH) ppm. Furthermore, no ^{31}P MAS NMR signal is detected in ZEO-4A or ZEO-4B (Fig. S14b), showing that all the organic structure-directing agent (OSDA) in the starting ZEO-2 material has been removed from the zeolite during the IChEZ reaction. This is corroborated by the ^{13}C and ^{31}P liquid NMR of the filtrate solution (Fig. S15), which shows that the OSDA can be recovered intact, which opens the way to its recycling. Self-supported FT-IR spectra on ZEO-4 also proved the silylation and OSDA removal during the IChEZ procedure (Fig. S16).

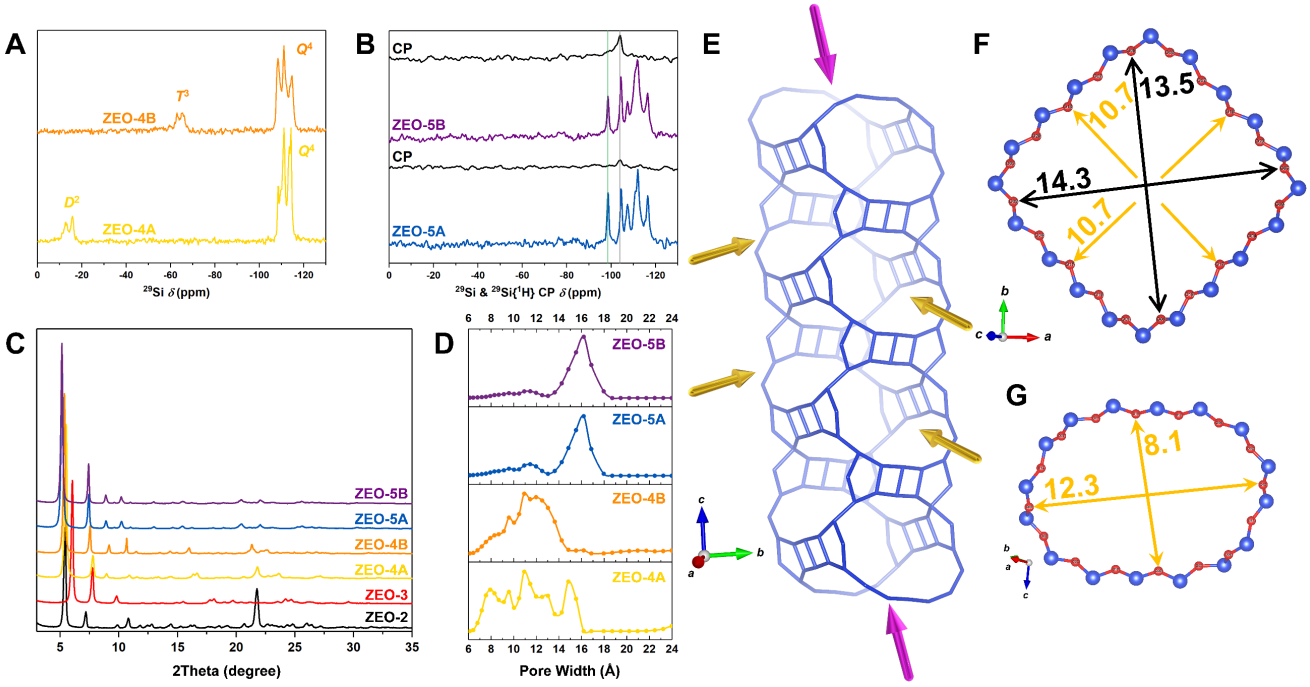

Fig. 2. Characterization of ZEO-4 and ZEO-5 and channel system and pore size of ZEO-5. (A, B) ^{29}Si MAS NMR spectroscopy: ZEO-4 materials (**A**) are interrupted frameworks containing either D^2 (ZEO-4A, yellow curve) or T^3 (ZEO-4B, orange curve) in addition to Q^4 but not Q^3. By contrast, ZEO-5 (**B**) coming from either ZEO-4A (blue curve) or ZEO-4B (violet curve) is a fully connected zeolite containing mainly Q^4 and just a minor concentration of Q^3 connectivity defects, highlighted by the grey vertical line, as proved by the poor intensity enhancement under cross-polarization (CP, black curves). The lowest field resonance around -98 ppm, not enhanced under cross-polarization, is highlighted by the green vertical line in the direct irradiation spectra (**B**) and is thus not a Q^3 but a Q^4, indicating very acute Si-O-Si angles around the corresponding Si atoms. **(C) Lab PXRD patterns:** 1D chain silicate ZEO-2, 1D-to-3D topotactically condensed zeolite ZEO-3, the interchain expanded interrupted zeolites ZEO-4A and ZEO-4B, and the fully connected zeolites obtained by calcination of the mentioned interrupted frameworks ZEO-5A and ZEO-5B, from bottom to top. **(D) Pore size distribution of ZEO-4 and ZEO-5,** calculated by NLDFT method from Argon adsorption isotherms (Fig. S13). **(E) 3D channel system in ZEO-5:** the 20 MR (purple arrows) of ZEO-5 are crossed by the 16MR (yellow arrows). **(F, G) The crystallographic clearance of 20 and 16 MR pores in Å:** black arrows show diagonal distances while yellow arrows show the distance between opposite sides of the pores; the van der Waals radius of O (2 × 1.35 Å) has been subtracted.

Preparation and structure of the true zeolite ZEO-5

Calcination of both variants of ZEO-4 produces the removal by combustion of the methyl groups and, through dehydration of adjacent Si-OH groups, a full connectivity of the newly introduced Si atoms yielding in both cases the same structure: the fully connected true zeolite ZEO-5 (Fig. 1D). Accordingly, the ^{29}Si MAS NMR spectra (Fig. 2B) contain only Q^4 silicon resonances and are essentially identical irrespective of the starting material, apart from minor differences in peak broadening and resolution (blue and violet curves). The small concentration of Q^3 resonances is demonstrated by the poor intensity enhancement under ^{29}Si{^{1}H} cross polarization (CP) conditions (black curves). A resonance at -98.6 ppm in the direct irradiation spectra (blue and violet curves), which is not enhanced under cross polarization, is at an unusually low field for a Q^4 Si site in SiO_2 zeolites (at least 6 ppm at a lower field than previous reports) but this is just due to the very sharp Si-O-Si angles at the responsible Si site, corresponding to an average angle of 126.3º according to the experimental relationship of Thomas et al.[14]

The single-crystal structure of ZEO-5 was also solved *ab initio* by using cRED. The cRED data were collected on the calcined crystals of both variants of ZEO-4 separately, and both resulted in *C*-centered monoclinic symmetry with a resolution of ~0.80 Å and more than 95% completeness (Fig. S7-S8, Tables S3-S4, and S6). The structures of calcined ZEO-5A and ZEO-5B were solved directly in the space group *C*2/*c*. Again, all the atoms, both silicon and oxygen, in the framework of the calcined materials were located directly from the observed electron density maps (Fig. S9). As stated above, the structure of the calcined zeolite, ZEO-5 (Fig. 1D), is unique irrespective of the starting ZEO-4 material and contains two fused double four-ring units that we call triple 4R (T4R). Such a structural unit has never been seen before in a zeolite, either natural or synthetic, regardless of chemical composition. The existence of T4R in ZEO-5 was double checked in the difference electron density map during the refinement against the high-quality cRED data (Fig. S9). The framework of ZEO-5 was refined anisotropically against the cRED data, and the refinement converged to an unweighted residual factor (R_1) value of 0.1139 and 0.1268 for the material obtained from ZEO-4A and ZEO-4B, respectively (Table S6). Further Rietveld refinement of the structure of ZEO-5 against SPXRD data was performed to obtain more precise bond lengths and angles (Fig. S11, Tables S12-S15). With the precise structural model in hand, we assign the -98.6 ppm resonance mentioned above to the Si atoms in the central 4R of the T4R (Si12 and Si13 with average Si-O-Si angles in the Rietveld refined structure of 137.5° and 137.0°, respectively). These average angles are less acute than expected according to the experimental equation mentioned above (126.3°) but it must be taken into account that these angles and chemical shifts are very much outside the range of experimental data used in determining the equation. The structural models derived by cRED and Rietveld refinement have been confirmed by STEM imaging (Fig. S12).

ZEO-5 properties

As a consequence of the formation of these T4R units, the 20 MR pores in ZEO-5 are no longer four-lobe shaped but are open through a rhomboid window with no protruding obstacles and with a much wider clearance (14.3×13.5 Å along the diagonals, 10.7×10.7 Å across opposite sides; Fig. 2F). On the other hand, the 16 MR pores along directions normal to [001] are open through oblong 12.3×8.1 Å windows (Fig. 2G), more open than those in the precursors, specially ZEO-4A (Fig. 1B-C, S17). Pore apertures of that size are unprecedented in stable, silica zeolites. Despite its very open framework ZEO-5 shows an outstanding stability that allows it to withstand calcination up to at least 1000 ºC and steaming under 10% H_2O up to at least 760 ºC, 3 hours (Fig. S1), which is a consequence of the full connectivity and silica composition of its framework.

Condensation of ZEO-4A and ZEO-4B into ZEO-5 results, paradoxically for a "condensation", in a significant expansion of the unit cell volume (12% and 7.5% expansion, respectively, Tab. S23), which is due to the longer size of the T4R unit compared to their precursors, *lau or D6R*, along the diagonals of the unit cell (Fig. 1), while the *c* parameter changes less than 0.5% as a result of the invariance of the basic ZEO-2 chain running along [001] in the zeolite. The new ZEO-5 zeolite holds the record for a low framework density silica polymorph (FD) at 11.08 Si atoms per nm^3, well below the prior record-holder, ZEO-3 (from which ZEO-5 is a σ-expansion, see Fig. 3), with FD = 12.76 Si nm^{-3}. This translates into a calculated density, 1.10 g cm^{-3}, which is almost that of water. Furthermore, among all the Zeolite Framework Types, irrespective of composition, connectivity or stability, included in the Database of Zeolite Structures,[15] only RWY has a lower framework density (7.6 T nm^{-3}). The RWY topology, containing 12-R pores and very large cages, is not a zeolite oxide but is only realized in UCR-20, a sulfide of gallium and germanium with an extremely poor thermal stability.[16] Other frameworks listed in the database with rings equal or larger than 18 MR and relatively low FD < 15 Si nm^{-3} are all interrupted frameworks and/or have a germanosilicate or phosphate composition, with inherently poor stability (Table S24). Because of its very open framework, ZEO-5 has unique textural properties (Fig 2D and S13, Tab. S16), compared to any reported zeolites. The BET surface area of ZEO-5A or ZEO-5B reached record-breaking values of 1533 or 1832 m^2/g, and the same is also true for their micropore volumes (0.40 or 0.38 cm^3/g).

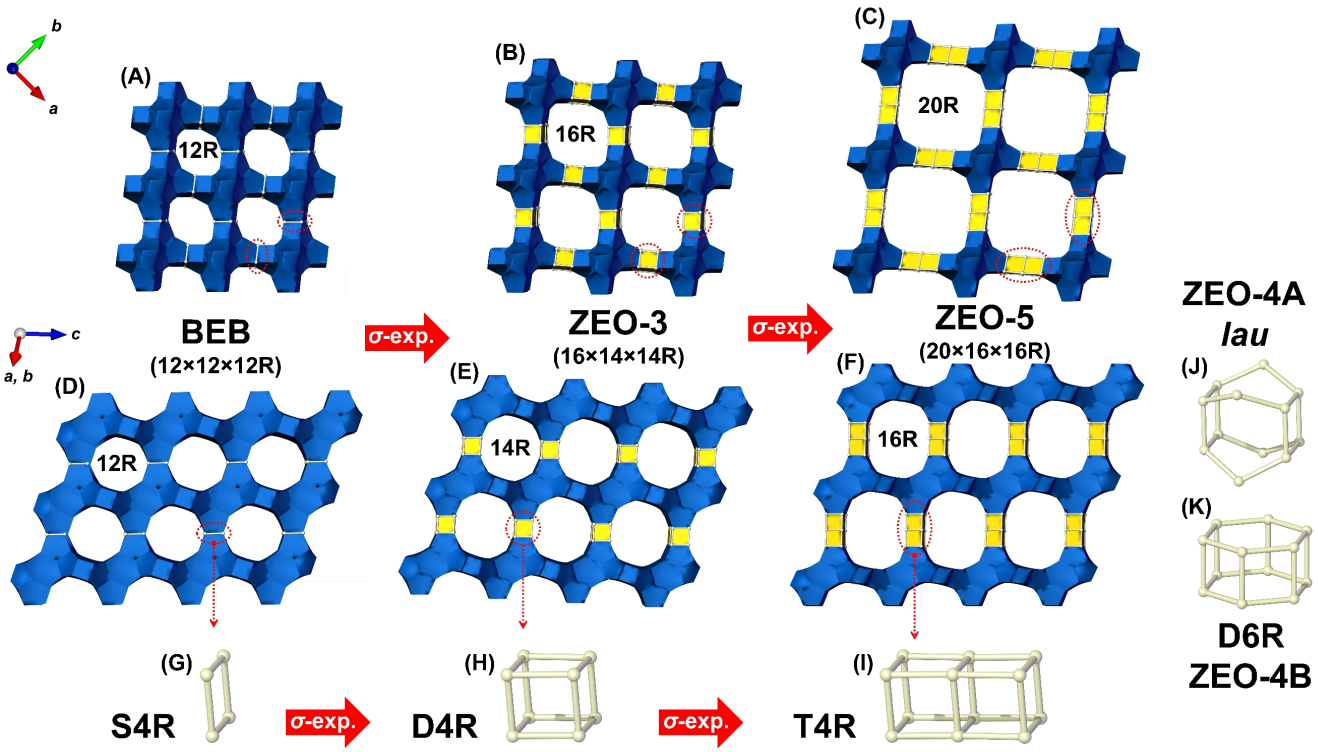

Fig. 3 Generation of extra-large pores by σ-expansion. A σ-expansion of polymorph B of the 3D large pore zeolite Beta (A, D), converts a S4R (G) into a double 4-ring (D4R, H) and generates the 3D extra-large pore ZEO-3 (B, E), while a σ-expansion of ZEO-3 converts a D4R into a T4R (I) and generates ZEO-5 (C, F), with even larger pores. The T4R derives by from the *lau* unit in ZEO-4A (J) or the D6R in ZEO-4B (K). The first of the σ-expansions mentioned (BEB to ZEO-3) is merely hypothetical, while the second one (ZEO-3 to ZEO-5) has some real meaning since ZEO-5 is made by the actual insertion of four Si atoms between the chains of the ZEO-3 precursor ZEO-2.

Introduction of heteroatoms and catalysis

We have introduced Ti atoms in ZEO-5 by a $TiCl_4$ vapor treatment (see SI) and compared the performance of the obtained Ti-ZEO-5 with that of Ti-Beta, the standard 3D large (12MR) pore Ti-zeolite catalyst, in the epoxidation of cyclooctene using both H_2O_2 and *tert*-butylhydroperoxide (TBHP) as oxidants. As shown in Table S25, the cyclooctene conversion of both zeolites is similar when using the small H_2O_2, but ZEO-5 provides a slightly higher intrinsic activity of Ti (turnover number). However, when the larger TBHP is used, the extra-large pore Ti-ZEO-5 shows a much better performance than Ti-Beta because of the easier diffusion along extra-large pores. More importantly, Ti-ZEO-5 is a promising catalyst for the industrially relevant clean production of propylene oxide (PO) through the epoxidation of propylene with cumene hydroperoxide (CHP) as oxidant, the so-called

CHPO process. As shown in Table S26, conventional microporous 10MR TS-1 and 12MR Ti-Beta are almost inactive in this reaction. However, Ti-ZEO-5, due to both its crystalline nature and its extra-large porosity similar to mesopores, demonstrates to be superior to the mesoporous Ti-HMS, the representative CHPO catalyst, in terms of site-time-yield of PO.

Lattice Energy of ZEO-5

As shown in Fig. S18, the structure of ZEO-5 has a calculated lattice energy of 30 kJ mol^{-1} of Si relative to quartz, significantly higher (~8 kJ mol^{-1}) than those calculated for all other known zeolites and also significantly larger than expected for its density (~6 kJ mol^{-1}). We ascribe this high energy to the stress inherent to the T4R unit, since it is known that even a D4R unit is much stressed for a pure silica composition.[17] ZEO-5 is actually at the edge of what Pophale et al. consider "feasible" (i.e. thermodynamically accessible) zeolites.[18] The realization of ZEO-5 emphasizes the idea that "unfeasible" structures can in fact be reached through alternative synthesis routes.[19,20]

Acknowledgements: SPXRD experiments were performed at the MSPD beamline bl04 at the ALBA Synchrotron with the collaboration of ALBA staff. We are thankful to C3UPO for providing HPC facilities.

Funding: Financial support from the Spanish Ministry of Science Innovation (PID2019-105479RB-I00 and TED2021-131223B-I00 projects, MCIN/AEI/10.13039/501100011033, and RYC2018-024561-I and FJC2018-035697-I grants, Spain), the National Natural Science Foundation of China (grant numbers: 22288101, 21920102005, 21835002, 22271115 and 52270111), the National Key Research and Development Program of China (grant numbers: 2022YFA1503600, 2021YFA1501202, 2021YFA1501401) the 111 project (B17020) and the Consejería de Universidades, Investigación e Innovación, Junta de Andalucía (grant number: POSTDOC_21_00069) are gratefully acknowledged. cRED data were collected at the Electron Microscopy Center (EMC), Department of Materials and Environmental Chemistry (MMK) in Stockholm University with the support of the Knut and Alice Wallenberg Foundation (KAW, 2012-0112) through the 3DEM-NATUR project. Additional funding from the European Union's Horizon 2020 research and innovation program under grant agreement No 823717-ESTEEM3 and the regional government of Aragon (DGA E13_20R) is also acknowledged. H.Y. is grateful to the China Scholarship Council for a PhD grant.

References

[1] Lin, Q.-F. et al. A stable aluminosilicate zeolite with intersecting three-dimensional extra-large pores. *Science* **374**, 1605–1608 (2021).
[2] Li, Jian. et al. A 3D extra-large-pore zeolite enabled by 1D-to-3D topotactic condensation of a chain silicate. *Science* **379**, 283–287 (2023).
[3] Morris, R. E. Clicking zeolites together. *Science* **379**, 236-237 (2023).
[4] Cundy, C. S. & Cox, P. A. The Hydrothermal Synthesis of Zeolites: History and Development from the Earliest Days to the Present Time. *Chem. Rev.* **103**, 663-702 (2003).
[5] Liebau, F. Nomenclature and Structural Formulae of Silicate Anions and Silicates. *Structural Chemistry of Silicates*, (Springer-Verlag, Berlin, 1985).
[6] Marler, B. & Gies, H. Hydrous layer silicates as precursors for zeolites obtained through topotactic condensation: a review. *Eur. J. Mineral.* **24**, 405-428 (2012).
[7] Roth, W.J., Nachtigall, P., Morris, R. E. & Čejka, J. Two-Dimensional Zeolites: Current Status and Perspectives. *Chem. Rev.* **114**, 4807−4837 (2014).
[8] Inagaki, S., Yokoi, T., Kubota, Y. & Tatsumi, T. Unique adsorption properties of organic–inorganic hybrid zeolite IEZ-1 with dimethylsilylene moieties. *Chem. Commun.* **48**, 5188–5190 (2007).
[9] Fan, W., Wu, P., Namba, S. & Tatsumi, T. A Titanosilicate That Is Structurally Analogous to an MWW-Type Lamellar Precursor. *Angew. Chem. Int. Ed.* **43**, 236–240 (2004).
[10] Ruan, J., Wu, P., Slater, B. & Terasaki, O. Structure Elucidation of the Highly Active Titanosilicate Catalyst Ti-YNU-1. *Angew. Chem. Int. Ed.* **44**, 6719-6723 (2005).
[11] Wu, P. et al. Methodology for Synthesizing Crystalline Metallosilicates with Expanded Pore Windows Through Molecular Alkoxysilylation of Zeolitic Lamellar Precursors. *J. Am. Chem. Soc.* **130**, 26, 8178–8187 (2008).
[12] Xu, L. & Sun, J. Recent Advances in the Synthesis and Application of Two-Dimensional Zeolites. *Adv. Energy Mater.* **6**, 1600441 (2016).
[13] Shamzhy, M., Gil, B., Opanasenko, M., Roth, W. J. & Čejka, J. MWW and MFI Frameworks as Model Layered Zeolites: Structures, Transformations, Properties, and Activity. *ACS Catal.* **11**, 2366–2396 (2021).
[14] Thomas, J. M., Klinowski, J., Ramdas, S., Hunter, B. K. & Tennakoon, D. T. B. The evaluation of non-equivalent tetrahedral sites from ^{29}Si NMR chemical shifts in zeolites and related aluminosilicates. *Chem. Phys. Let.* **102**, 158-162 (1983).
[15] Ch. Baerlocher & L.B. McCusker, Database of Zeolite Structures, http://www.iza-structure.org/databases/ (accessed 03/23/2023)
[16] Zheng, N., Bu, X., Wang, B. & Feng, P. Microporous and Photoluminescent Chalcogenide Zeolite Analogs. *Science* **298**, 2366-2369 (2002).
[17] Zicovich, C. M., Gándara, F., Monge A. & Camblor, M.A. In Situ Transformation of TON Silica Zeolite into the Less Dense ITW: Structure-Direction Overcoming Framework Instability in the Synthesis of SiO2 Zeolites, *J. Am. Chem. Soc.* **132**, 3461–3471 (2010).
[18] Pophale, R., Cheeseman, P. A. & Deem, M. W. A database of new zeolite-like materials. *Phys. Chem. Chem. Phys.* **13**, 12407-12412 (2011).
[19] Eliášová, P. et al. The ADOR mechanism for the synthesis of new zeolites. *Chem. Soc. Rev.* **44**, 7177 (2015).
[20] Mazur, M. et al. Synthesis of 'unfeasible' zeolites. *Nat. Chem.* **8**, 58–62 (2016).